

RETINAL MACULAR EDEMA SEVERITY DETECTION BASED ON RADIAL SYMMETRY DEPEND NN CLASSIFIER

Parvathi I.N*

Mrs V.Virjin Sonia **

Abstract:

Diabetic macular edema (DME) is an advanced symptom of diabetic retinopathy and can lead to irreversible vision loss. In this paper, a two-stage methodology for the detection and classification of DME severity from color fundus images is proposed. DME detection is carried out via a supervised learning approach using the normal fundus images. A feature extraction technique is introduced to capture the global characteristics of the fundus images and discriminate the normal from DME images. Exudates are one of the visible signs of diabetic retinopathy and a marker for the presence of coexistent retinal edema. Automatic exudates detection would be useful in order to detect and treat diabetic retinopathy in an early stage. In this project a method for automatic detection of optic disc followed by classification of hard exudates pixels in retinal image. Optic disc localization is achieved by Radial symmetry transform (RST) to identify initial set of candidate regions followed by connected component analysis to locate the actual optic disc. Exudates are detected using hidden neural network based classifier. The sensitivity, specificity and accuracy are used to evaluate the performance.

Index terms: Abnormality detection, diabetic macular edema, hard exudates,

* M.E in vins Christian college of engineering

** Asst.prof. in vins Christian college of engineering

I. INTRODUCTION

Macular edema may occur due to the swelling in the macular region of retina. Diabetic-related eye diseases are the most common cause of blindness in the world. The most effective treatment for these eye diseases are early detected through regular screenings. During the screening, color retinal images are obtained using fundus camera[17]. Diabetic retinopathy is one of the most serious complications of diabetics. The earliest sign of diabetic retinopathy are damage to blood vessels in the eye and then formation of lesions in retina.[4]. An unhealthy abnormal fundus images usually exhibit some abnormalities, one of which is the presence of exudates/lesions. Exudates /lesions are typically random whitish/yellowish patches of varying sizes, shapes and locations[15].The Macula is a very small area at the center of retina. It is a thin layer of light sensitive tissues that lines the back of the eye. Macula edema develops when blood vessels in the retina are leaking fluids. The macula does not function properly when it is swollen. Also, this macula is the part of the retina responsible for sharp vision due to its high density of cone photoreceptors.Diabetic macular edema caused due to diabetics is high risk complication,which can cause irreversible loss of vision[1]-[3]. An unhealthy abnormal fundus image usually exhibit some abnormalities, one of which is the presence of exudates/lesions [15].Hard exudates are formed due to secreation of plasma from capillaries resulting from the complication of retinal vasculature and could lead to retinal swelling. In color fundus image, hard exudates may appear as yellow-white deposit. Detecting the presence of hard exudates in different area of retina is the standard method to assess DME [1],[4],[5]. Severity of the risk of edema is evaluated based on proximity of hardexudate to the macula.DME can be detected directly or indirectly. Direct way makes use of stereoscopy or optical computed tomography image. Indirect method is by detecting the presence of hard exudates in retina[3].Two stage methodology for the assessment of DME. The first stage is to determine the presence or absence of hard exudates. Once, the presence is detected, the second stage is to measure the risk of exhibiting the hard exudates.

II.PAST WORK

Direct detection of edema is based on the estimate of height map of the macula[2]. The estimated height map is noisy and mean height difference is demonstrated between the height maps of normal and abnormal fundus image. Local scheme that perform localization of hard

exudates or hard exudates clusters[10] and global schemes for detecting the presence/absence of hard exudates in images.

a) *Local schemes*

The goal of local scheme is to detect maximum number of hard exudates. The most common approach to process the green channel of color fundus image is thresholding the intensity histogram. Background suppression is the approach that is used to find the hard exudates candidates. Background estimation include median filtering[27], morphological operations[19], and clustering[11]. Edge detection can be used for identifying the candidate pixels.

b) *Global schemes*

Features such as visual word/group using a dictionary have to represent color fundus image as normal or abnormal[25]. SIFT features of keypoints representing the hard exudate and multiscale AM-FM features have been used to construct visual words. Creation of visual vocabulary requires clustering local regions into words/group.

III PROPOSED METHOD

Dark structure that is roughly at the center of retina is known as macula. Hard exudate appear as clusters of bright, high contrast lesions and are usually well localized. For normal retina there is a rough symmetry about the macula in the circular region twice the diameter of optic disc. Using this feature describe normal and abnormal case. In order to describe the relevant feature, first obtain the color fundus image. Then circular region of interest have been extracted. The intermediate representation of I_{MP} is known as motion of pattern of ROI. Relevant features of I_{MP} is derived to classify the given image as normal and abnormal.

1) *Region of interest*

Severity of the risk is based on the location of hard exudate clusters relative to the macula. The best fit circle within the fundus mask with macula at the center of given image. The region within the circle is known as ROI. The green channel of I form input to all processing. The center of the macula is automatically detected. Optic disc may have brightness

characteristics similar to hard exudate and it is detected and masked. So the resulting image contain circular patches indicating macula and rectangular patch indicate optic disc.

2) Generation of motion pattern

The generation of motion pattern is motivated by the effect of motion on biological/computer vision system. These system represent a scene as a set of of spatially sampled intensities or an image. when object in a scene moves at a high speed, it usually leaves a smearing pattern in captured image. In computer vision, the estimation and removal of smear pattern is known as motion blur in images. Signal aggregation at sensor location in human eye and camera, give rise to smearing effect. In order to simulate this effect, induce motion in a given image to generate a sequence of image. A motion pattern for I_{MP} for i is derived as

$$I_{MP}(\vec{r}) = f(G_N(I(\vec{r}))) \quad 1$$

Where \vec{r} denotes a pixel location, G_N is a transformation representing the induced motion. G_N generates N transformed images which are combined using f to coalesce the sampled intensities at each location. $G_n(I)$ represented as

$$G_N(i) = \{R_{\theta_n}(I)\} \quad 2$$

In the problem at hand, since HE appear as bright localized lesions against the retinal background, they should form a bright smear pattern in I_{MP} whereas the textured background will be smoothed out.

3) Feature Selection

The motion pattern I_{MP} generated by inducing motion I on results in the smearing of lesions when present, along the motion path .To effectively describe this motion pattern,a descriptor derived from the Radon space. The radon transform can be represented as

$$P_\alpha(r) = \int_{-\alpha}^{\alpha} \int_{-\alpha}^{\alpha} f(x, y) \delta(r - x \cos \alpha - y \sin \alpha) dx dy \quad 3$$

Where α is the angle between the line and y axis.. The image I_{MP} is projected to obtain a vector response for every angle α and the desired feature vector then is derived by concatenating the

responses for different orientations. The spatial extent of any HE that may be present, is enhanced in the motion pattern I_{MP} and is in turn reflected immediately in the projection based feature vector. Thus, the feature vector for an abnormal retina will have several peaks in its profile due to intensities corresponding to HE. On the other hand, the feature vectors for a normal retina will have relatively uniform values resulting in a compact normal subspace. These feature vectors are used for learning the subspace corresponding to normal images.

4) *Abnormality detection- learning normal class*

Learning normal cases is achieved using single class classification. In this approach, a classification boundary is formed in the feature space around the subspace corresponding to normal cases. If a new image, when transformed to this feature space, lies within this boundary, then it is classified as normal and abnormal otherwise. Simple classifier known as neural network classifier can be used. In neural network linear subspace can be defined for the normal case.

5) *Determining the severity of macular edema*

Assessing the severity of macular edema is the next task. Here, the macular region which is the circular ROI within 1 optic disc diameter from the center, is of key interest as any HE within this region indicates high risk for DME, requiring immediate attention. The macula in a normal image is relatively darker than other regions in the fundus image and is characterized by rotational symmetry. This symmetry information to establish the risk of exhibiting edema: good degree of symmetry is taken to indicate the abnormality is not inside macula and hence it is declared as a moderate case. Asymmetry of the macula on the other hand implies abnormality is within the macula and hence the case is deemed severe. A method to detect severity of edema based on rotation symmetry has also been used earlier where the symmetry of larger ROI centered on the macula is considered [33]. A slightly different approach by considering the symmetry of only the macular region. Unlike [33], removal of blood vessels is not required here, as visibly large vasculature is usually not observed within macula in color fundus image. A symmetry measure is defined as the second norm of the distance between the histograms of diametrically opposite pair of patches. Here eight angular samples were used to create eight patches from the circular ROI and a histogram of 10 bins was computed for every patch. Since

the intensities corresponding to HE contribute mostly to the higher bins in the histogram, only the last five bins are used for measuring the symmetry. A threshold on the symmetry measure is used for assessing the degree of abnormality of an image as moderate or severe risk of DME. Let μ and σ be the maximum and minimum symmetry values for *normal* images in the training set used for abnormality detection. Then the severity of a given abnormal image is determined by comparing the symmetry measure of this image against a threshold as follows. It is desirable to set the threshold to be a percentage of the maximum symmetry value for normal images. It is desirable to select a low value for σ to achieve highest classification accuracy for the severe class of DME images as they require immediate medical attention.

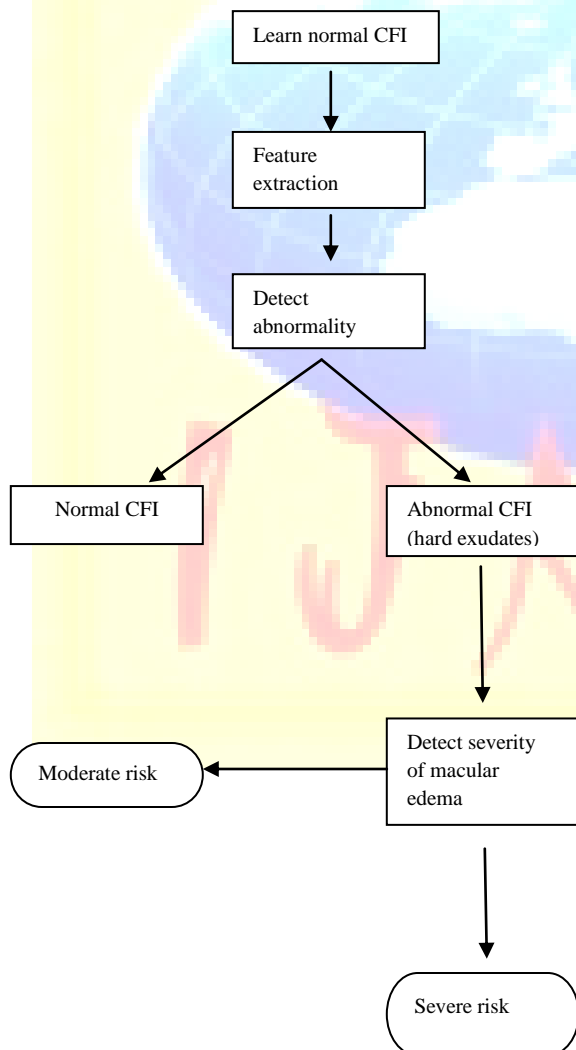


Fig.1.Proposed system architecture

IV EXPERIMENTS AND RESULTS

The experiments for assessing the proposed method were performed on four publicly available datasets of color fundus images. A set of experiments were first conducted to determine the optimal motion parameters. Next, using these results, the method was assessed on the datasets and compared with existing algorithms for DME detection.

A. Dataset

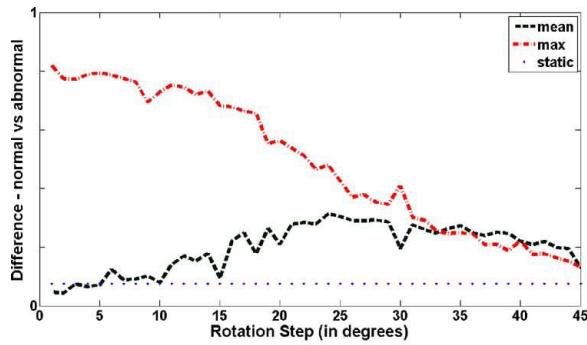
Four publicly available datasets were used for validating the proposed method. The first two of the four datasets described next have associated annotations at image level for DME. The *DMED* or *HEI-MED* dataset comprises of compressed (Jpeg) images where 68 fundus images not exhibiting any signs of a disease whereas 54 fundus images contain HE. These images are acquired from patients of different ethnicity and age group. Consequently, a large variability is observed across images in color and tissue pigmentation. 18 (of the 68) normal images were randomly selected and used for creating the normal subspace while the remaining images were used for testing the performance of the method. The abnormal images with no signs of hard exudates were excluded from the experiments.

B. Motion Parameter Estimation

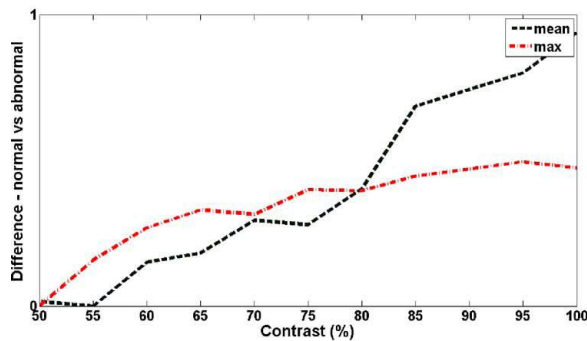
The discriminability between normal and abnormal retinal images is contingent on the right choice of parameters when inducing motion in the static image. Two parameters govern the rotational motion: the rotation step (in degrees) which controls the sampling rate at each location and the function used for coalescing the samples. In order to determine the optimal parameters, a normal retinal image was created by averaging the green channel of 400 retinal images from *MESSIDOR* dataset. No preprocessing was performed in order to retain all variations in intensity bias that occur in practice. Only a circular region of interest centered at macula and with radius of two optic disc diameter was used in the experiments for simplicity. An abnormal retinal image

was synthesized from the averaged normal retina by adding a localized circular structure with high contrast, to model an HE lesion. Rotational motion was induced on the modeled normal and abnormal images using both *mean* and *maximum* as the coalescing function. Presence of lesion in the abnormal image results in smearing of lesion intensities over the motion path in the motion pattern. This effect of lesion on retinal background can be observed as change in local information with respect to the motion pattern of normal retina.

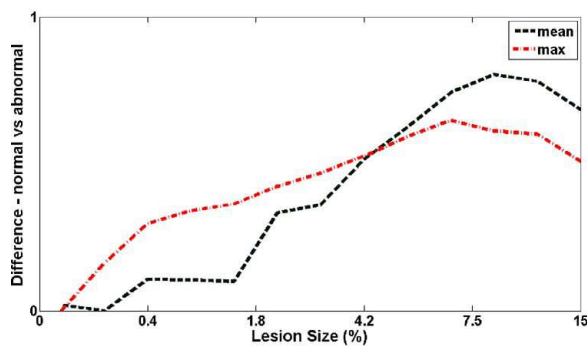
- 1) 1) Effect of Rotation Step and Coalescing Function on Class Discriminability: A set of plots of as a function of motion parameter and lesion size and contrast for one complete rotation and for two choices for the coalescing function.
- 2) 2) Effect of Lesion Size and Contrast on Class Discriminability: Next, observe the effect of lesion size as the percentage of ROI and lesion contrast with respect to the retinal background for the selected rotation step and the coalescing function. As HE clusters also appear at various contrast and sizes, observe the effect of changing these two parameters by fixing the rotation. The values based on the observation of HE clusters in MESSIDOR. The discriminability is higher initially for the *maximum* rather than the *mean* coalescing function for low lesion contrast, but this effect is reversed as the lesion contrast increases [see Fig. 9(b)].



(a)



(b)



(c)



Similar behavior is also observed with increasing lesion size on discriminability of normal and abnormal retina [see Fig. 9(c)]. Based on these observations, we conclude that using *maximum* as coalescing function enables better detection of lesions. even when they are small and have low local contrast. Therefore the suggested motion parameter values can be used on retinal images irrespective of the size and resolution of the ROI selected.

C. Detection of Macular Edema

Based on the above experimental findings, the motion parameters and coalescing function were chosen for the assessment of the proposed method. The coalescing function of maximum was chosen and three rotation step sizes, 1, 3 and 5 were considered. Since the optic disc is also a bright, albeit large structure, it was masked out before inducing motion. A descriptor based on Radon transform described earlier was computed with a resolution of 30.

D. Classification of Macular Edema Cases

Finally, the effect of the threshold (T) (on rotational symmetry metric) in severity assessment is studied. The results for different threshold settings on the images detected as abnormal for MEDDIDOR dataset. The threshold is expressed as a percentage of the symmetry measure of normal ROIs used in the abnormality detection task. It can be seen that the classification accuracy is high when the value of is at 25% of the value for normal. The classification accuracy for the moderate class falls as the value of is increased to 75%. This implies that of the normal ROI is sensitive to intensity variations but does not affect the classification accuracy of severe cases.

V. CONCLUDING REMARKS

This project proposed and evaluated a method for DME detection and assessment. The significant contributions of this work are: 1) a hierarchical approach to the problem, 2) a novel representation for the first level, to classify an image as normal/abnormal (containing HE), and 3) a rotational asymmetry measure for the second level, to assess the severity of risk of DME. The novel representation captures the global image characteristics. Such global features have not been used successfully earlier for HE detection. In the first level, a supervised technique based on learning the image characteristics of only normal patients is used for detecting the abnormal cases pertaining to HE. In the second level, the severity of the abnormality is assessed by analyzing the rotational asymmetry of the macular region in retina.

VI. REFERENCES

- [1] L. Giancardo, F. Meriaudeau, T. P. Karnowski, Y. Li, K. W. Tobin, Jr., and E. Chaum, "Automatic retina exudates segmentation without a manually labelled training set," in *Proc. 2011 IEEE Int. Symp. Biomed. Imag: From Nano to Macro*, Mar. 2011, pp. 1396–1400.
- [2] L. Giancardo, F. Meriaudeau, T. Karnowski, K. Tobin, E. Grisan, P. Favaro, A. Ruggeri, and E. Chaum, "Textureless macula swelling detection with multiple retinal fundus images," *IEEE Trans. Biomed. Eng.*, vol. 58, no. 3, pp. 795–799, Mar. 2011.
- [3] M. R. Hee, C. A. Puliafito, C. Wong, J. S. Duker, E. Reichel, B. Rutledge, J. S. Schuman, E. A. Swanson, and J. G. Fujimoto, "Quantitative assessment of macular edema with optical coherence tomography," *Arch. Ophthalmol.*, vol. 113, no. 8, pp. 1019–1029, Aug. 1995.
- [4] J. Davidson, T. Ciulla, J. McGill, K. Kles, and P. Anderson, "How the diabetic eye loses vision," *Endocrine*, vol. 32, pp. 107–116, Nov. 2007.
- [5] J. Davidson, T. Ciulla, J. McGill, K. Kles, and P. Anderson, "How the diabetic eye loses vision," *Endocrine*, vol. 32, pp. 107–116, Nov. 2007.
- [6] C. P. Wilkinson, F. L. Ferris, R. E. Klein, P. P. Lee, C. D. Agardh, M. Davis, D. Dills, A. Kampik, R. Pararajasegaram, and J. T. Verdager, "Proposed international clinical diabetic retinopathy and diabetic macular edema disease severity scales," *Am. Acad. Ophthalmol.*, vol. 110, no. 9, pp. 1677–1682, Sep. 2003.
- [7] R. F. N. Silberman, K. Ahlrich, and L. Subramanian, "Case for automated detection of diabetic retinopathy," *Proc. AAAI Artif. Intell. Development (AI-D'10)*, pp. 85–90, Mar. 2010.
- [8] M. Verma, R. Raman, and R. E. Mohan, "Application of tele ophthalmology in remote diagnosis and management of adnexal and orbital diseases," *Indian J. Ophthalmol.*, vol. 57, no. 5, pp. 381–384, Jul. 2009.
- [9] M. D. Abramoff, M. Niemeijer, M. S. Suttorp-Schulten, M. A. Viergever, S. R. Russell, and B. van Ginneken, "Evaluation of a system for automatic detection of diabetic retinopathy from color fundus photographs in a large population of patients with diabetes," *J. Diabetes Care*, vol. 31, no. 2, pp. 193–198, Nov. 2007.
- [10] S. Philip, A. Fleming, K. Goatman, S. Fonseca, P. McNamee, G. Scotland, G. Prescott, P. F. Sharp, and J. Olson, "The efficacy of automated disease/no disease grading for diabetic

- retinopathy in a systematic screening programme,” *Br. J. Ophthalmol.*, vol. 91, no. 11, pp. 1512–7, Nov. 2007.
- [10] H. Jaafar, A. Nandi, and W. Al-Nuaimy, “Detection of exudates in retinal images using a pure splitting technique,” in *Proc. Annu. Int. Conf. IEEE Eng. Med. Biol. Soc. (EMBC)*, Aug. 2010, pp. 6745–6748.
- [11] P. C. Siddalingaswamy and K. G. Prabhu, “Automatic grading of diabetic maculopathy severity levels,” in *Int. Conf. Syst. Med. Biol. (ICSMB)*, Dec. 2010, pp. 331–334.
- [12] C. I. Sanchez, M. Garca, A. Mayo, M. I. Lopez, and R. Hornero, “Retinal image analysis based on mixture models to detect hard exudates,” *Med. Image Anal.*, vol. 13, no. 4, pp. 650–658, Aug. 2009.
- [13] A. Osareh, M. Mirmehdi, B. Thomas, and R. Markham, “Automated identification of diabetic retinal exudates in digital colour images,” *Br. J. Ophthalmol.*, vol. 87, pp. 1220–1223, Oct. 2003.
- [14] T. Walter, J.-C. Klein, P. Massin, and A. Erginay, “A contribution of image processing to the diagnosis of diabetic retinopathy-detection of exudates in color fundus images of the human retina,” *IEEE Trans. Med. Imag.*, vol. 21, no. 10, pp. 1236–1243, Oct. 2002.
- [15] H. Wang, W. Hsu, K. G. Goh, and M. L. Lee, “An effective approach to detect lesions in color retinal images,” in *Proc. IEEE Conf. Comput. Vis. Pattern Recognit.*, 2000, vol. 2, pp. 181–186. [16] W. Hsu, P. Pallawala, M. L. Lee, and K.-G. A. Eong, “The role of domain knowledge in the detection of retinal hard exudates,” in *Proc. 2001 IEEE Comput. Soc. Conf. Comput. Vis. Pattern Recognit. (CVPR 2001)*, 2001, vol. 2, pp. II-246–II-251.
- [17] C. Sanchez, A. Mayo, M. Garcia, M. Lopez, and R. Hornero, “Automatic image processing algorithm to detect hard exudates based on mixture models,” in *Proc. 28th Annu. Int. Conf. IEEE Eng Med. Biol. Soc.*, Sep. 2006, pp. 4453–4456.
- [18] Y. Hatanaka, T. Nakagawa, Y. Hayashi, Y. Mizukusa, A. Fujita, M. Kakogawa, K. K.M. D. , T. Hara, and H. Fujita, “Cad scheme to detect hemorrhages and exudates in ocular fundus images,” in *Proc. SPIE Med. Imag. 2007: Comput.-Aided Diagn.*, Mar. 2007, vol. 6514, pp. 2M1–2M8.

- [19] S. Ravishankar, A. Jain, and A. Mittal, "Automated feature extraction for early detection of diabetic retinopathy in fundus images," in *IEEE Conf. Comput. Vis. Pattern Recognit.*, Jun. 2009, pp. 210–217.
- [20] A. Osareh, B. Shadgar, and R. Markham, "A computational- intelligence- based approach for detection of exudates in diabetic retinopathy images," *IEEE Trans. Inf. Technol. Biomed.*, vol. 13, no. 4, pp. 535–545, Jul. 2009.
- [21] H. Li and O. Chutatape, "A model-based approach for automated feature extraction in fundus images," in *Proc. 9th IEEE Int. Conf. Comput. Vis.*, Oct. 2003, vol. 1, pp. 394–399.
- [22] M. Garcia, R. Hornero, C. Sanchez, M. Lopez, and A. Diez, "Feature extraction and selection for the automatic detection of hard exudates in retinal images," in *Proc. 29th Annu. Int. Conf. IEEE Eng. Med. Biol. Soc.*, Aug. 2007, pp. 4969–4972.
- [23] K. Ram and J. Sivaswamy, "Multi-space clustering for segmentation of exudates in retinal color photographs," in *Proc. Annu. Int. Conf. IEEE Eng. Med. Biol. Soc.*, Sep. 2009, pp. 1437–1440.
- [24] A. Rocha, T. Carvalho, S. Goldenstein, and J. Wainer, Points of interest and visual dictionary for retina pathology detection Inst. Comput., Univ. Campinas, Tech. Rep. IC-11-07, Mar. 2011.
- [25] C. Agurto, V. Murray, E. Barriga, S. Murillo, M. Pattichis, H. Davis, S. Russell, M. Abramoff, and P. Soliz, "Multiscale am-fm methods for diabetic retinopathy lesion detection," *IEEE Trans. Med. Imag.*, vol. 29, no. 2, pp. 502–512, Feb. 2010.
- [26] N. P. Ward, S. Tomlinson, and C. J. Taylor, "Image analysis of fundus photographs. the detection and measurement of exudates associated with diabetic retinopathy," *Ophthalmology*, vol. 96, no. 1, p. 86-6, Jan. 1989.
- [27] W. Huan, H. Wynne, and L. M. Li, "Effective detection of retinal exudates in fundus images," in *Proc. 2nd Int. Conf. Biomed. Eng. Informat.*, Oct. 2009, pp. 1–5.
- [28] J. Singh, G. D. Joshi, and J. Sivaswamy, "Appearance-based object detection in colour retinal images," in *Proc. Int. Conf. Image Process.*, 2008, pp. 1432–1435.
- [29] G. D. Joshi, J. Sivaswamy, K. Karan, and S. R. Krishnadas, "Optic disk and cup boundary detection using regional information," in *Proc. Int. Conf. Image Process.*, 2010, pp. 948–951.

- [30] J. V. Stone, "Object recognition using spatiotemporal signatures," *Vision Research*, vol. 38, no. 7, pp. 947–951, Apr. 1998.
- [31] S. Cho, Y. Matsushita, and S. Lee, "Removing non-uniform motion blur from images," in *Proc. IEEE 11th Int. Conf. Comput. Vis.*, Oct. 2007, pp. 1–8.
- [32] S. Nishida, J. Watanabe, I. Kuriki, and T. Tokimoto, "Human visual system integrates color signals along a motion trajectory," *Current Biol.*, vol. 17, no. 4, pp. 366–372, Feb. 2007.
- [33] K. S. Deepak, G. D. Joshi, and J. Sivaswamy, "Content-based retrieval of retinal images for maculopathy," in *Proc. 1st ACM Int. Health Inf. Symp.*, 2010, pp. 135–143.
- [34] MESSIDOR, Jun. 2011 [Online]. Available: <http://messidor.crihan.fr/index-en.php>
- [35] DIARETDB0, DIARETDB0: Evaluation database and methodology for diabetic retinopathy algorithms May 2007 [Online]. Available: <http://www2.it.lut.fi/project/imageret/diaretdb0/>
- [36] DIARETDB1, May 2009, DiaRetDB1: Diabetic retinopathy database and evaluation protocol [Online]. Available: <http://www2.it.lut.fi/projec/imageret/diaretdb1/>

BIBILOGRAPHY



NAME: Parvathi I N

I have passed my M.sc software Engineering (five years integrated)degree from Noorul Islam College of Engineering during the acedamic year 2010-2011.Now Iam doing my M.E programe in vins christain college of Engineering.I have Participated in International conference at Maria Engineering college, Atoor and National Conference at Bharathiyar Institute of Engineering for Women, Salem, India